33RD INTERNATIONAL COSMIC RAY CONFERENCE, RIO DE JANEIRO 2013
THE ASTROPARTICLE PHYSICS CONFERENCE

ICRC 2013

Search for cosmic-ray antideuterons with BESS-Polar II

K. YOSHIMURA[1,*] K. ABE[2,†], H. FUKE[3], S. HAINO[1,‡], T. HAMS[4,§], M. HASEGAWA[1], A. HORIKOSHI[1], K. C. KIM[5], A. KUSUMOTO[2], M. H. LEE[5], Y. MAKIDA[1], S. MATSUDA[1], Y. MATSUKAWA[2], J. W. MITCHELL[4], J. NISHIMURA[6], M. NOZAKI[1], R. ORITO[2,§], J. F. ORMES[7], K. SAKAI[4,§], M. SASAKI[4,§], E. S. SEO[5], R. SHINODA[6], R. E. STREITMATTER[4], J. SUZUKI[1], K. TANAKA[1], N. THAKUR[4], T. YAMAGAMI[3], A. YAMAMOTO[1], T. YOSHIDA[3],

[1] *High Energy Accelerator Research Organization (KEK), Tsukuba, Ibaraki 305-0801, Japan*
[2] *Kobe University, Kobe, Hyogo 657-8501, Japan*
[3] *Institute of Space and Astronautical Science, Japan Aerospace Exploration Agency (ISAS/JAXA), Sagamihara, Kanagawa 229-8510, Japan*
[4] *NASA-Goddard Space Flight Center (NASA-GSFC), Greenbelt,MD 20771, USA*
[5] *IPST, University of Maryland, College Park, MD 20742, USA*
[6] *The University of Tokyo, Bunkyo, Tokyo 113-0033, Japan*
[7] *University of Denver, Denver, CO 80208, USA*
[*] *now at: Okayama University*
[†] *now at: ICRR, Tokyo*
[‡] *now at: National Central University*
[§] *also at: Center for Research and Exploration in Space Science and Technology (CRESST)*
[¶] *now at: Tokushima University*

yosimura@okayama-u.ac.jp

Abstract: High precision cosmic-ray antiproton fluxes recently reported by BESS-Polar and PAMELA are consistent with secondary production from interactions of primary cosmic rays with the interstellar medium. This severely constrains the possibility of antiprotons of primary origin such as annihilation of supersymmetric dark matter or evaporation of primordial black holes. In the case of antideuterons, however, secondary production in collisions is strongly suppressed, especially at low energies, because of the very low production cross-section and strict kinematic requirements compared to antiproton production. The lack of secondary background would imply that there is still plenty of room to search for primary antideuterons from novel production processes. In spite of such attractive features, antideuterons detection is enormously challenging since the expected flux is extremely small and superior particle identification is necessary to separate antideuteron candidates from the antiproton background. The most sensitive reported search used BESS flight data obtained during the previous solar minimum period in 1997. By comparison, the BESS-Polar II flight in 2007/2008 accumulated cosmic-ray data in near solar minimum conditions with more than ten times the statistics of BESS97. We will report the result of a new search for antideuterons with unprecedented sensitivity using BESS-Polar II.

Keywords: Cosmic-ray antideuteron, BESS-Polar, Superconducting spectrometer, Solar minimum

1 Introduction

Cosmic-ray antiprotons ($\bar{p}$'s) have been unique probe to investigate elementary particle phenomena in the early universe and to study fundamental cosmic-ray processes, e.g. production, propagation, and solar modulation. This is primarily because most of $\bar{p}$'s are produced in primary cosmic-ray interactions with the interstellar medium (so-called "secondary $\bar{p}$'s") and the flux can be well-predicted by various theoretical models. [1, 2, 3, 4, 5]. Novel primary origins, if they exist, would exhibit themselves as flux enhancement over the secondary antiproton spectrum. Many experimental programs have been measuring $\bar{p}$'s and pursuing their origins. The data from BESS '95 and '97 taken in the last solar minimum period showed flatter $\bar{p}$ spectrum towards low energy, which might suggest the existence of a primary origin[6]. Data reported recently from both PAMELA and BESS-Polar II[7, 8], however, showed good consistency with secondary $\bar{p}$'s.

Cosmic-ray antideuterons ($\bar{d}$'s)@are in a different situation. Thanks to their heavier mass, the probability of production in cosmic-ray interaction is much smaller, especially at low energies, because of the very low production cross-section and strict kinematical requirement. So one single $\bar{d}$ event would be a direct evidence of novel primary origins[9, 10] However, expected flux is extremely small and numerous $\bar{p}$'s become severe background to identify $\bar{d}$'s. An experiment with large exposure factor and good particle identification devices is necessary to investigate $\bar{d}$'s. As such, few searches have been carried out so far and no $\bar{d}$ candidate was observed yet. The best limit was reported by the BESS experiment obtained during last solar minimum period[11].

There are several on-going and future program which could further investigate $\bar{d}$'s[12, 13, 14]. BESS-Polar II, second long duration flight over antarctica, was carried out in 2007/8 and data analysis is proceeded. The data taken during 24.5 scientific observation provide a good opportunity to search for $\bar{d}$ especially in the low energy region since the flight was performed in the solar minimum period as well as entirely in the low geomagnetic cutoff region. We could expect great improvement over the last reported data from the BESS experiment. In this paper, current status on analysis to search for $\bar{d}$ will be described.

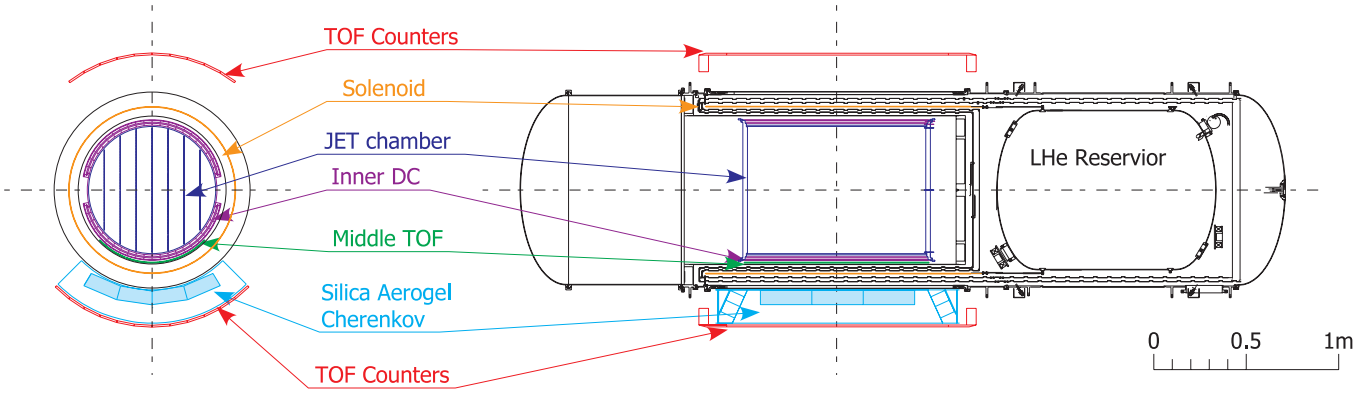

Figure 1: Cross sectional view of BESS-Polar II instrument.

2 BESS-Polar II Instrument and Flight

Figure 1 shows a cross-sectional view of the BESS-Polar II instrument. A uniform field of 0.8 T is produced by a thin superconducting solenoid, and the field region is filled with tracking detectors. Cylindrical coaxial geometry realize a large acceptance of 0.23 m^2sr. Tracking is performed by fitting up to 48 hit points in drift chambers (JET) and 4 hit points in inner drift chambers (IDC), resulting in a magnetic-rigidity($R \equiv Pc/Ze$) resolution of 0.4% at 1 GV, and a maximum detectable rigidity (MDR) of 270 GV. The upper and lower scintillator hodoscopes provide time-of-flight (TOF) and dE/dx measurements as well as trigger signal . The timing resolution of each hodoscope is 120 ps, resulting in a β^{-1} resolution of 2.5%. The instrument also incorporates a threshold-type Cherenkov counter with a silica aerogel radiator with refractive index $n = 1.03$ (ACC) that can reject e^- and μ^- backgrounds by a factor of 12000. The threshold rigidities for $\bar{p}$ (p) and $\bar{d}$ (d) are 3.8 GV and 7.6 GV, respectively. In addition, a thin scintillator middle-TOF (MTOF) is installed between the central tracker and the solenoid to detect low energy particles which cannot penetrate the magnet wall. The timing resolution of these hodoscopes is 320 ps.

The BESS-Polar II flight was carried out in December 2007 through January 2008. The payload was launched on December 23 from Williams Field near the US McMurdo Station in Antarctica and circulated around the South Pole for 29.5 days. Data were taken for live-time periods of 1286460 seconds at altitudes of 34 km to 38 km (residual air of 5.8 g/cm^2 on average). The cutoff rigidity was kept under 0.6 GV for the entire flight trajectory. 4.7×10^9 cosmic-ray events were accumulated without any online event selections as 13.6 terabytes of data recorded in the hard disk drives. During the 24.5 days of observation, all detectors operated well and they exhibited the expected performance except for the central tracker. The JET chamber showed an instability due to high-voltage fluctuation. However more than 90% of the data has been successfully calibrated while keeping sufficient tracker quality, a task that was realized by development of time-dependent tracker calibration.

3 Data Analysis

Data analysis on $\bar{d}$ is basically same as that used for $\bar{p}$ measurements as described in [17]. The major difference

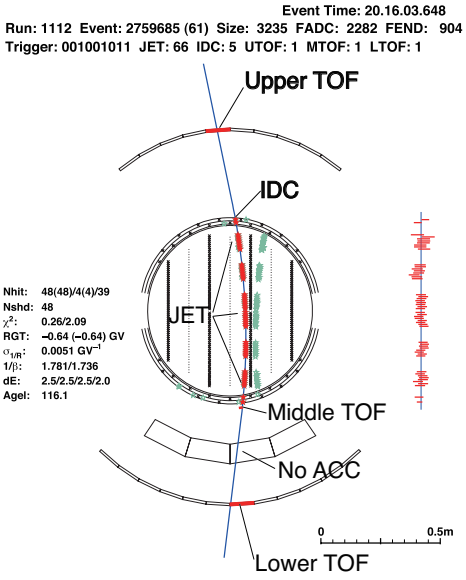

Figure 2: Event display of one of $\bar{p}$ candidate

is that in $\bar{p}$ analysis relativistic particles ($e\mu\pi$) are main background sources, however $\bar{p}$'s are now background to identify $\bar{d}$.

For clear detection of $\bar{d}$ over numerous $\bar{p}$'s background, we optimize the selections to ensure reliable information on rigidity and β measurement. Special cares are taken to reduce tails of distributions, which were caused by scattering, interaction, and accidental tracks etc. In these studies we used positive samples (proton and deuteron) as well as $\bar{p}$'s with mask of $\bar{d}$'s region.

After iterative tuning the selections, we performed a new search for $\bar{d}$'s as describe below.

3.1 Clean single track selection

As a first step, clean single track events are selected as shown in Figure 2. The following two stages of the selections are applied:

pre-selection

Select non-interacting particles which pass through the fiducial region by using JET number-of-hit information, the TOF number of hits, Track position,

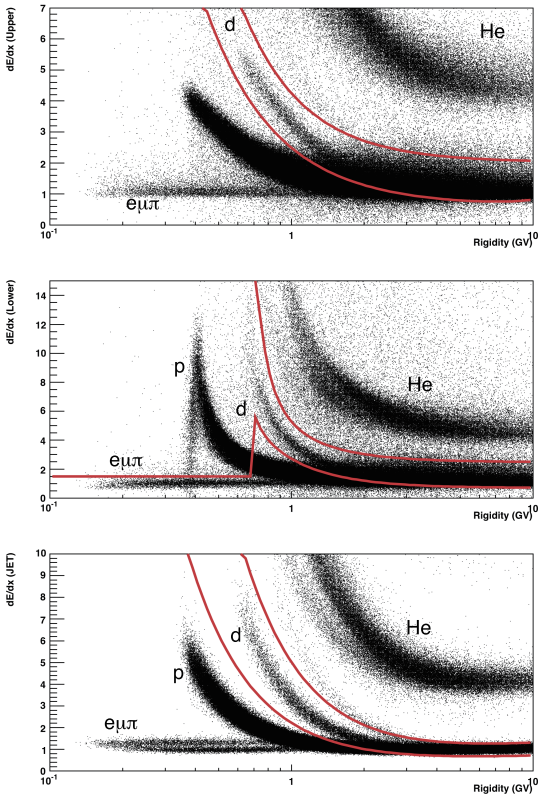

Figure 3: dE/dx vs rigidity plots for upper TOF (top), lower TOF (middle), and JET chamber (bottom), respectively. The curves in each plot define dE/dx band cut position.

etc. The surviving events are used for starting samples to be used for later analysis.

track quality cut

The various cuts are then applied to ensure the quality of the track along with correct timing information by using χ^2 of the track fitting , consistency between track and TOF hit information, number of z-hit information from IDC, etc. These cuts also eliminate hard scattered events. We also apply the cuts to reject large number of extra hits in the tracker, which are occasionally caused by accidental incident and might cause mis-measurement of tof timing and dE/dx information.

3.2 Deuteron and Antideuteron selection

Then we extract $\bar{d}$ (and d) signals using combination of dE/dx, ACC information. At this point, the same selection criteria for positive and negative curvature events are applied under the assumption that non-interactive $\bar{d}$ behaves like d except for their deflection thanks to the cylindrical symmetry of the BESS-Polar spectrometer. We can also estimate various efficiencies for $\bar{d}$'s using positive curvature events (d).

We first apply band selections according to dE/dx for upper and lower TOF and JET chamber. Figure 3 shows dE/dx vs. rigidity plot for each detector. We require that $\bar{d}$'s as well as d's must have the dE/dx inside the "dE/dx" band shown in Figure 3. In the low rigidity region, this

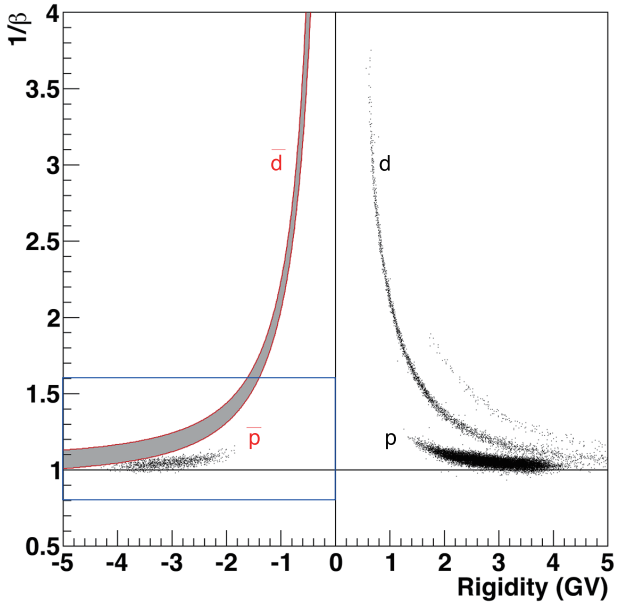

Figure 4: β^{-1} vs. rigidity plot for the samples after the dE/dx and the ACC cut.

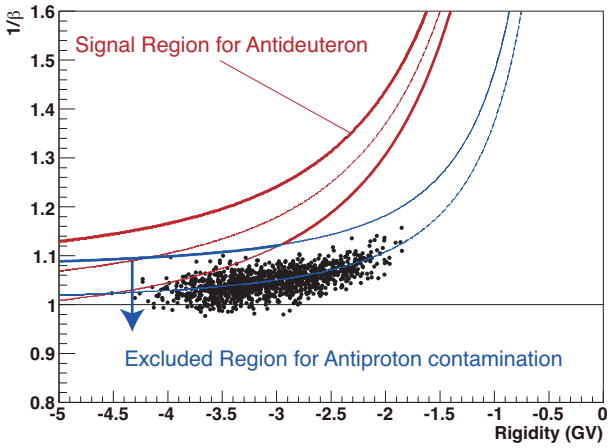

Figure 5: Closeup view of the box shown in Figure 4. The red and blue curves show signal and excluded region, respectively. No $\bar{d}$ candidate was found in the signal region.

dE/dx cut rejects most of e/μ/π, p and $\bar{p}$, and all of the particles with charge greater than 1. The ACC veto cut is then applied to reject relativistic e/μ/π samples as well as p's and $\bar{p}$'s having rigidity higher than threshold ($E > 3.8$ GV).

3.3 Mass selection

Figure 4 shows the scatter plot of β^{-1} vs. rigidity after the dE/dx and the ACC cut. Clear band structures are visible, each of which corresponds to particle mass as $m = R\sqrt{1/\beta^2 - 1}$. By applying the dE/dx cut, most of the particles are eliminated except for the d ($\bar{d}$). The curves are shown to define a 3σ band from the center of the β^{-1} distribution for d samples. In the negative rigidity side,

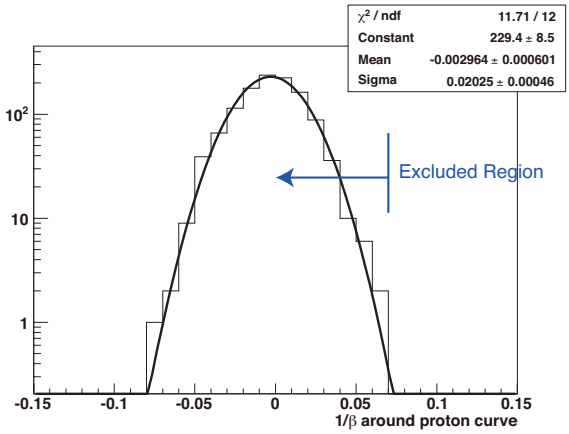

Figure 6: β^{-1} deviation from the center of $\bar{p}$ distribution for all negative events.

$\bar{d}$ region was masked for blind analysis at this stage. We can clearly observe $\bar{p}$ remnant survived from dE/dx and ACC cuts in the just opposite side of the proton remnant. We carefully study the properties of these remnants and iteratively optimize the selection criteria to clean up their distribution, i.e. remove tail.

3.4 Signal and Excluded region

To perform a $\bar{d}$ search, we define $\bar{d}$ signal region and $\bar{p}$ excluded region as follows:

$\bar{d}$ signal region

Inside 3 σ band from the center of $\bar{d}$ distribution (masked in Figure 4)

$\bar{p}$ excluded region

The excluded region for $\bar{p}$ contamination was determined such that we only expect 0.1 event or less pbar contamination in the $\bar{d}$ signal region. Expected number of background was calculated under assumption that β^{-1} distribution is gaussian. Here we set the boundary at 3.5 σ away from the center of $\bar{p}$ distribution.

3.5 Search for Antideuterons

Finally, we open the $\bar{d}$ signal region. Figure 5 shows the closeup view of the negative rigidity side in Figure 4. The search box is already open. Also shown in Figure 6 is β^{-1} distribution from the center of $\bar{p}$ distribution for all negative particles. No $\bar{d}$ candidate was not observed in the signal region (w/ $\bar{p}$ exclusion). It is clearly seen that β^{-1} distribution shows nearly gaussian distribution as we assumed and no significant tail.

4 Summary

Using BESS-Polar II, we performed $\bar{d}$ search. We have optimized selection criteria and signal region so that the expected number of background is 0.1 event or less. No $\bar{d}$ candidate was not observed and resultant upper limit of $\bar{d}$ flux will be report soon.

Acknowledgements

The authors thank NASA Headquarters for the continuous encouragement in this U.S.-Japan cooperative project. Sincere thanks are expressed to the NASA Balloon Programs Office at GSFC/WFF and CSBF for their experienced support. They also thank ISAS/JAXA and KEK for their continuous support and encouragement. Special thanks go to the National Science Foundation (NSF), U.S.A., and Raytheon Polar Service Company for their professional support in U.S.A. and in Antarctica. The BESS-Polar experiment is being carried out as a Japan-U.S. collaboration, and is supported by a KAKENHI(13001004,18104006, and 22540322) in Japan, and by NASA in U.S.A.

References

[1] T. Mitsui, Ph.D. thesis, the University of Tokyo (1996).
[2] J. W. Bieber *et al.*, Phys. Rev. Lett. **83**, 674 (1999); Proc. 26th Int. Cosmic Ray Conf. (Utah) **7**, 17 (1999).
[3] L. Bergström *et al.*, Astrophys. J. **526**, 215 (1999).
[4] F. Donato *et al.*, Astrophys. J. **563**, 172 (2001).
[5] V. S. Ptuskin *et al.*, Astrophys. J. **642**, 902 (2006).
[6] S. Orito *et al.*, Phys. Rev. Lett. **84**, 1078 (2000).
[7] O. Adriani *et al.*, Phys. Rev. Lett. **105**, 121101 (2010);
[8] K. Sakai *et al.*, Proc. 32nd Int. Cosmic Ray Conf. (Beijing) , (2011); K. Sakai, Ph. D Thesis, The University of Tokyo , (2011).
[9] F. Donato *et al.*, Proc. 30th Int. Cosmic Ray Conf. (Merida) , (2007).
[10] P. Salati *et al.*, Particle Dark Matter: Observations, Models and Searches (Cambridge University Press) , 521 (2010).
[11] H. Fuke *et al.*, Phys. Rev. Lett. **95**, 081101 (2005);
[12] J.W. Mitchell *et al.*, Proc. 31th Int. Cosmic Ray Conf. (Lodz) , (2009).
[13] V. Choutke *et al.*, Proc. 30th Int. Cosmic Ray Conf. (Merida) **4**, 765 (2007).
[14] C.J. Hayley *et al.*, Adv. Spac. Res. , (2011).
[15] A. Yamamoto *et al.*, Adv. Spac. Res. , (2011).
[16] K. Yoshimura *et al.*, Proc. 31th Int. Cosmic Ray Conf. (Lodz) , (2010).
[17] K. Abe *et al.*, Phys. Lett. B **670**, 103 (2008).